LIMNOLOGY
and
OCEANOGRAPHY

ASLO

Limnol. Oceanogr. 9999, 2019, 1–15

doi: 10.1002/lno.11256

Light exposure along particle flowpaths in large rivers

John R. Gardner [1*,a] **Scott H. Ensign,** [2] **Jeffrey N. Houser,** [3] **Martin W. Doyle** [1]

[1]Nicholas School of the Environment, Duke University, Durham, North Carolina
[2]Stroud Water Research Center, Avondale, Pennsylvania
[3]USGS-Upper Midwest Environmental Sciences Center, La Crosse, Wisconsin

Abstract

Sunlight is a critical resource in aquatic systems driving photosynthesis, photodegradation of organic matter and contaminants, animal behavior, and the activity of human pathogens. In rivers, solutes, materials, and organisms are turbulently mixed across the water column during downstream transport and exposed to highly variable sunlight. However, there are no measurements of suspended particles' sunlight exposure during downstream transport to characterize this variability, and it is unclear if current measurement approaches and optical theory capture the light exposure of suspended particles. We deployed neutrally buoyant drifters and stationary buoys in the Upper Mississippi (WI, U.S.A.) and Neuse Rivers (NC, U.S.A.) to measure underwater sunlight from the perspective of suspended particles. In our study sites, underwater sunlight varied more along flowpaths measured by drifters than over time measured by fixed-site buoys; sunlight exposure along flowpaths was dominated by bursts of light (sunflecks) that accounted for 62–99% of the cumulative sunlight exposure; and modeled sunlight exposure using optical theory was consistently 56–1700% higher than measured sunlight exposure along flowpaths. Our results suggested that suspended particles in the study reaches experienced darker conditions than predicted and have important implications for how to quantify underwater sunlight in rivers.

The amount of sunlight transmitted through water is critical for aquatic ecosystems. Sunlight drives photosynthesis (i.e., photosynthetically active radiation [PAR]), photodegradation of organic matter and contaminants (i.e., ultraviolet radiation [UV]), animal behavior, and the activity of human pathogens (Kirk 1994; Wetzel 2001; Leech and Johnsen 2009; Vähätalo 2010; Cory et al. 2014; Nelson et al. 2018). The sunlight that is transmitted downward through water is called downwelling solar irradiance, but hereafter is referred to as light for simplicity. The amount of light at a particular time and depth, in the water column or on the riverbed, can be estimated by measuring or modeling light at the water surface $E_d(0)$, typically corrected for surface reflection, and assuming light decreases exponentially with depth (Davies-Colley et al. 1984; Gordon 1989; Kirk 1994; Davies-Colley and Nagels 2008);

$$E_d(z) = E_d(0)e^{-K_d z} \quad (1)$$

where E_d is the downwelling light (i.e., solar irradiance in μmol m^{-2} s^{-1} of PAR, lumens m^{-2}, or watts m^{-2}), z is the depth below the water surface (m), and K_d is the diffuse attenuation coefficient for downwelling light (m^{-1}).

Optical theory, Eq. 1, is useful for modeling underwater light at a particular location and time; however, when applying this theory to model the light exposure of suspended particles, it assumes that measurements from a fixed-site translate into light exposure along Lagrangian flowpaths. Here, flowpath refers to the position of a neutrally buoyant particle over time within the three-dimensional space of a river. For example, in rivers, the light exposure of a population of phytoplankton vertically mixed through the water column is often modeled as the depth-averaged mean light exposure (E_{mean}) assuming instantaneous mixing across a mixing depth (z_m), or the mean water depth in a river, combined with measurements of light at the water surface and light attenuation from fixed-sites (Eq. 2) (Mallin and Paerl 1992; Phlips et al. 2000; Sellers and Bukaveckas 2003; Ochs et al. 2013). While representative of a mean condition, this approach does not account for the variability in light.

$$E_{mean} = \frac{E_d(0)\left(1 - e^{-K_d z}\right)}{K_d z_m} \quad (2)$$

Rivers present a challenge in modeling the light exposure of suspended particles during downstream transport. The terms in

*Correspondence: johngardner87@gmail.com

[a]Present address: Department of Geological Sciences, University of North Carolina, Chapel Hill, North Carolina

Additional Supporting Information may be found in the online version of this article.

Eqs. 1, 2 are potentially variable over space and time. The amount of light that reaches the water surface is affected by external "filters" such as topography, riparian shading, channel geometry, and atmospheric conditions (DeNicola et al. 1992; Davies-Colley and Quinn 1998; Julian et al. 2008*a*,*b*). Light attenuation through the water column is affected by internal light filters that scatter and absorb light in water such as concentrations of chromophoric dissolved organic matter (CDOM), suspended sediment, and phytoplankton (Davies-Colley 1990; Smith et al. 1997; Wetzel 2001). The depth of a suspended particle is controlled by turbulent mixing across the depth of a river, and both mixing and river depth can vary with flow conditions and channel morphology (Leopold and Maddock 1953; Reynolds et al. 1991; Rutherford 1994). Light exposure may therefore depend upon the particular flowpath through a river—vertically, laterally, and longitudinally (Sverdrup 1953; Reynolds 1990; Reynolds et al. 1991; Köhler et al. 2018). However, there are no Lagrangian measurements that follow a particle downstream to understand light variability, and it is unclear if current measurement approaches and optical theory capture the light exposure of suspended particles in rivers.

A useful analogy is to compare the light exposure of a suspended particle during downstream transport with a plant on the forest floor under a canopy of trees. The forest floor has dim, diffuse light punctuated by unpredictable, brief periods of direct light known as "sunflecks" (Chazdon 1988; Chazdon and Pearcy 1991; Leakey et al. 2004). Sunflecks have been defined as continuous periods of time above a threshold light value (typically PAR = 10–100 μmol m^{-2} s^{-1}). Measurement approaches and the ecological importance of sunflecks are well established in forest ecology (Pearcy and Way 2012; Way and Pearcy 2012), and increasingly in stream ecology (Wellnitz and Rinne 1999; Hillebrand 2005; Hall et al. 2015; Heaston et al. 2017), and the same concepts could be applied to suspended particles in rivers as they are exposed to highly variable light.

Matching the spatial–temporal scales of light measurements with timescales of biological response is needed to inform a physiological-based approach to river ecosystems. Plants, including phytoplankton, respond to rapid changes in light (Chazdon and Fetcher 1984; Falkowski 1984; Reynolds 1990). Fluctuating light conditions, compared to constant conditions, can affect photosynthetic efficiency and trigger physiological adaptations in individuals (Mallin and Paerl 1992; Litchman 2000; Köhler et al. 2018). At the community level, phytoplankton community structure can change depending on the temporal pattern in light (Litchman 1998). Yet, it remains unclear how phytoplankton populations persist in large, optically deep rivers where the photic depth is less than the water depth (Sellers and Bukaveckas 2003; Koch et al. 2004; Walks 2007; Ochs et al. 2013). Resolving this question is crucial because at the ecosystem level, phytoplankton can be the dominant carbon source in riverine food webs (Thorp et al. 1998; Thorp and Delong 2002; Doi 2009) and can account for a large portion of the primary production in large river ecosystems (Descy and Gosselain 1994; Thorp and Delong 1994; Reynolds 2006).

To better understand underwater light in large rivers from the perspective of suspended particles, we collected high frequency light measurements in two rivers using neutrally buoyant, Lagrangian drifters and stationary buoys (Fig. 1). The drifters measured light along downstream flowpaths while the stationary buoys collected light over time at multiple depths and locations. Our specific objectives were to (1) characterize the frequency, magnitude, and duration of sunflecks to help future work parameterize the variability in light exposure of suspended particles, (2) estimate the relative variation in light along flowpaths (i.e., as seen by suspended organisms) vs. fixed sites (i.e., as seen by organisms rooted to the riverbed), and (3) evaluate how well fixed-site measurements and optical theory model the light exposure of suspended particles compared to flowpath measurements. Our questions were:

1. What is the frequency, duration, and magnitude of sunflecks along flowpaths?
2. How does light variability along flowpaths compare to light variability over time at fixed-sites?
3. How well do fixed-site measurements and optical theory model the light exposure along downstream flowpaths?

We predicted that (1) the variability in light is greater along flowpaths than over time at a fixed-sites, and (2) that fixed-site

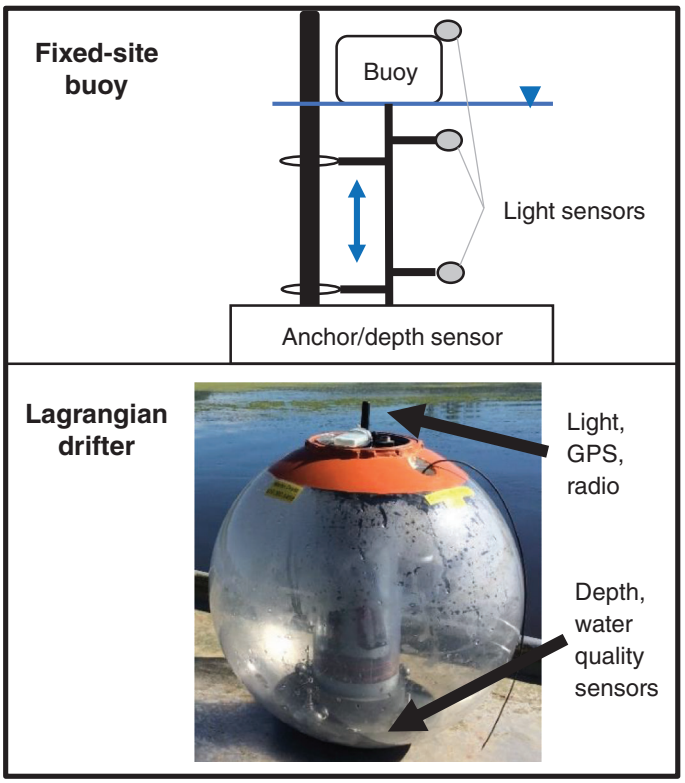

Fig. 1. Diagram of a fixed-site buoy and photo of a neutrally buoyant drifter (Hydrosphere, Planktos Instruments). [Color figure can be viewed at wileyonlinelibrary.com]

measurements and optical theory do not capture spatial–temporal heterogeneity in light conditions and vertical mixing and therefore will either over or under predict the light exposure of suspended particles.

Methods

Study sites

We collected data from the 8th order Upper Mississippi River (UMR) near La Crosse, Wisconsin during summer 2016 and the 5th order Neuse River (NR) in North Carolina from 2014 to 2016 (Fig. 2). The UMR is a large, floodplain river that is punctuated by a series of navigational locks and dams forming impoundments, navigational pools, backwaters, and secondary channels (Wilcox et al. 1993). On the UMR, we focused on secondary channels in an 11 km section of Navigational Pool 8. The mean discharge was 1266 m^3 s^{-1} during our study and the widths of the main and secondary channels are 500 m and 10–350 m, respectively. On the NR, we focused on a 40 km reach immediately upstream of the estuary with a mean discharge of 156 m^3 s^{-1} during our study. The NR has a single channel (~ 100 m) that meanders through the coastal plain before rapidly fanning out in width (~ 2000 m) at the estuary.

Light measurements

We measured illuminance, the light visible to the human eye, in units of lux (lumens m^{-2}) as a proxy for biologically important light spectra such as PAR. Despite differences in spectral range and response between lux and PAR sensors, our measurements (Supporting Information Fig. S1) as well as previous studies show strong empirical relationships between lux and PAR (Long et al. 2012), indicating lux is an appropriate proxy. In addition, it was not mechanically possible to install PAR sensors on the drifters. Therefore, we used lux sensors (HOBO Pendant, Onset, Massachusetts, U.S.A., minimum detection limit = 10 lx) on all drifters and fixed-site buoys. All measurements are of downwelling light (i.e., upward facing sensors), the most commonly measured light vector (Vähätalo 2010), but note suspended particles may receive light from all directions (Kirk 1994).

Drifter data collection

We measured light along flowpaths using Lagrangian, neutrally buoyant drifters (HydroSphere, Planktos Instruments, LLC, Morehead City, North Carolina, U.S.A.) (Ensign et al. 2017). Drifters were ballasted so that the light sensors were facing up while the water quality sensors and pressure transducers were always facing down (Fig. 1). Each drifter collected light, depth, and tilt angle vertically (i.e., accelerometer) every 0.5 min in the NR and 2 min in the UMR. Drifters were adjusted for neutral buoyancy immediately prior to deployment based on the water temperature and salinity. While the drifters were ballasted, they could tilt in response to strong currents. Therefore, light measurements were cosine corrected for the tilt angle from vertical;

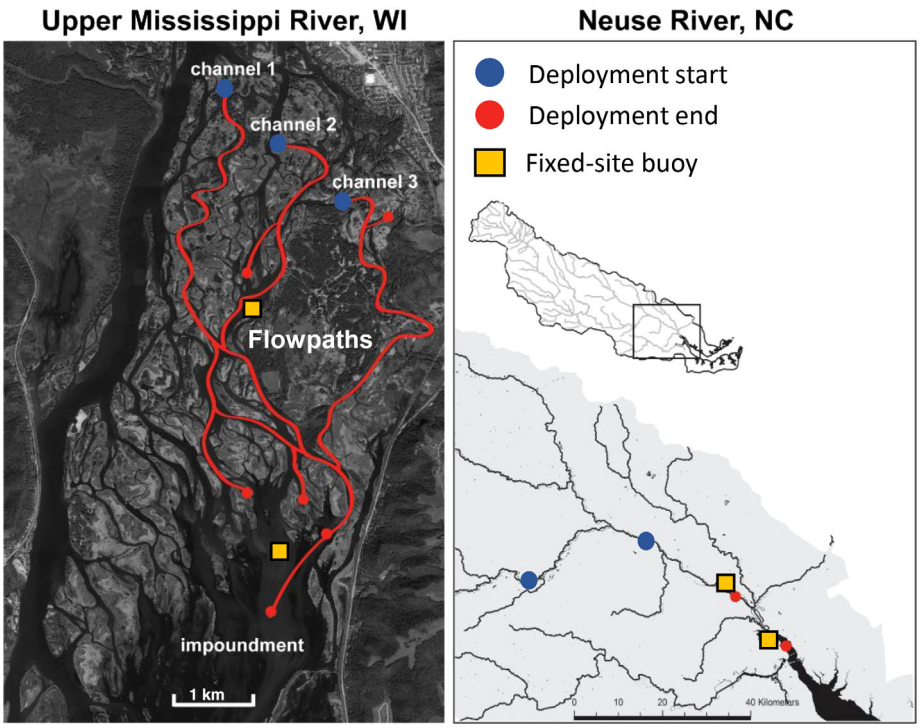

Fig. 2. Map of the study sites, the UMR pool 8 in Wisconsin, U.S.A. and the NR in North Carolina, U.S.A. The lines show the typical tracks of drifters through the UMR. The large dots are the typical deployment coordinates and the small dots are the typical recovery coordinates. The squares are the locations of fixed-site buoys. [Color figure can be viewed at wileyonlinelibrary.com]

$$E_d = E_{meas} \cos\theta \quad (3)$$

where E_d is the corrected downwelling light (lux), E_{meas} is the measured downwelling light (lux), and θ is the tilt angle with respect to the vertical axis. The median tilt angle was 8° and most measurements (96%) were less than 25° (Supporting Information Fig. S2). The cosine-correction increased light by < 1% at a tilt angle of 8° and < 10% at 25° (Supporting Information Fig. S2); therefore, the difference between measured and cosine-corrected values was relatively small. However, all drifter light measurements presented here were cosine-corrected.

In the NR, we completed six deployments using one drifter, with three deployments spanning two consecutive days; therefore, nine total deployment-days. In the UMR, one to three drifters were deployed over eight different dates with 16 deployment-days in total (Table 1). In the UMR, deployments were limited to 8 h due to downstream dams, and deployments were limited to 24 h on the NR to ensure recovery. During two deployments on the NR, drifters entered the estuary after a full 24 h and 43 km of downstream travel. Deployments spanned a wide range of discharge conditions in the NR from low summer flow (83% exceedance probability) to an overbank flood (0.04% exceedance probability). Deployments on the UMR occurred during one summer and over a narrow range of flow conditions (Table 1). While deployments occurred during different seasons in the NR, we treated deployments as replicates and do not discuss seasonality.

The drifters typically followed the channel thalweg and traveled 1.2–43 km at an average downstream velocity of 0.11–0.98 m s^{-1} across deployments (Table 1). Twenty-one of the 25 deployment-days (84%) successfully collected neutrally buoyant, Lagrangian data (i.e., uninhibited movement in the water column during the duration of deployment), while five deployments did not due to trapping on submerged wood jams, retention in backwater eddies, or user error. Three of the successful deployments experienced 10–60 min of trapping on wood jams. When possible, we removed drifters from wood jams and eddies for continued data collection. Deployment periods that were not Lagrangian were removed prior to data analysis; therefore, some deployment records have data gaps or were entirely omitted from analysis.

Drifters were not a perfect analog for suspended particles (e.g., phytoplankton, DOM) in turbulent fluids. The drifters

Table 1. Summary of drifter deployments including river discharge, distance traveled, deployment duration, and mean velocity measured by drifters. Dashes denote the second day of the same deployment.

River	Date	River discharge (m^3 s^{-1})	Drift distance (km)	Drift time (h)	Mean velocity (m s^{-1})
UMR	08 Jun 2016	1665	8.2	7	0.33
UMR	16 Jun 2016	1314	9.4	7.5	0.34
UMR	23 Jun 2016	1311	7.7	7.0	0.32
UMR	23 Jun 2016	1311	6.6	7.5	0.25
UMR	28 Jun 2016	1382	8.3	5.5	0.48
UMR	28 Jun 2016	1382	8.4	5.0	0.46
UMR	28 Jun 2016	1382	1.2	0.5	0.11
UMR	29 Jun 2016	1390	2.6	6.3	0.13
UMR	29 Jun 2016	1390	3.5	7.3	0.17
UMR	05 Jul 2016	1065	8.3	7.0	0.33
UMR	05 Jul 2016	1065	5.2	5.0	0.30
UMR	11 Jul 2016	821	6.5	6.3	0.29
UMR	11 Jul 2016	821	5.7	6.0	0.27
UMR	14 Jul 2016	1068	5.4	6.5	0.23
UMR	14 Jul 2016	1068	3.5	6.5	0.16
UMR	14 Jul 2016	1068	2.1	3.0	0.19
NR	25 Sep 2014	94	43.0	23.0	0.52
NR	26 Sep 2014	102	—	—	—
NR	10 Mar 2015	365	17.0	4.8	0.98
NR	16 Jun 2015	28	11.5	8.3	0.39
NR	17 Jun 2015	24	—	—	—
NR	12 Oct 2015	212	36.3	25.5	0.55
NR	13 Oct 2015	212	—	—	—
NR	10 Apr 2016	73	8.2	5.0	0.47
NR	21 Apr 2016	69	5.3	6.0	0.47

are 0.4 m diameter spheres and likely responded only to turbulent eddies with characteristic length scales ≥ 0.4 m (Rutherford 1994; D'Asaro et al. 1996). Lagrangian drifters used in oceans are typically 1–2 m and have been shown to track turbulent motions equal to or greater than their size (D'Asaro et al. 1996; D'Asaro 2003; Lien and D'Asaro 2006). The largest scale of turbulence in a river is typically limited by depth (Rutherford 1994; Nadaoka and Yagi 1998; Jirka 2001) which was 1–10 m in our study reaches. Therefore, the largest turbulent eddies were 2–20 times greater than the drifter size, indicating our drifters can respond to multiple scales of turbulence. Based on our depth time series presented in "Results" section, the spatial scale of interest (1–40 km along a river), and previous drifter studies, our drifters captured the mean flowpath and low frequency variability in depth experienced by a neutrally buoyant particle. Therefore, the drifters were an effective proxy for the variability in light seen by suspended particles along a mean flowpath.

Drifter light attenuation

We estimated longitudinal patterns in K_d at a spatial resolution of hundreds of meters using drifter measurements of light and depth. Light attenuation is traditionally estimated by measuring light across a vertical profile, then rearranging Eq. 1 so that K_d (m^{-1}) is the slope of the linear regression of light vs. depth, $E_d(0)$ (lux) is the y-intercept, and z (m) is depth (Davies-Colley et al. 1984; Kirk 1994).

$$\log(E_d) = K_d z + \log(E_d(0)) \quad (4)$$

In contrast to fixed-site sampling, drifters move passively through the water column sampling light at various depths, geographic locations, and times across the river reach. In our deployments, this provided hundreds of paired light-depth measurements along river reaches up to 40 km to fit Eq. 4. The entire drifter deployment during daylight hours could be used to estimate a temporally and spatially reach-integrated K_d (Supporting Information Fig. S3). Rather than presenting a reach-integrated K_d, we instead present a spatially explicit K_d along a reach by binning time windows over which we can assume a constant surface light using a rolling window of 30 min. A 30-min window was chosen as a compromise between assumptions of constant surface light and having enough data points to fit Eq. 4 (n = 13 in UMR, n = 58 in NR due to sampling frequency). Nonsignificant fits ($p > 0.1$) were removed as well as spurious K_d with positive slopes, likely due to variable surface light. The standard error of the slope of the linear regression of light vs. depth for each window (Eq. 4) was used as a proxy for uncertainty in K_d. The standard error provides an empirical measurement of uncertainty reflective of the conditions over which K_d was estimated.

Fixed-site data collection

We compared the variability in underwater light measured by drifters with underwater light measured by fixed-site buoys. Buoys were placed in upstream and downstream sites spaced 3 km and 20 km in the UMR and NR reaches, respectively (Fig. 2). Buoys were equipped with three upward facing light sensors (HOBO pendant, Onset, Massachusetts, U.S.A.) placed just above the air–water interface, 0.5 m, and 1–1.5 m below the water surface as well as a pressure transducer (HOBO, Onset, Massachusetts, U.S.A.) fixed to an anchor on the riverbed to measure water depth (Fig. 1).

The buoy was anchored in place but was able to rise and fall so that depth with respect to the water surface was constant over time. In the NR, the buoys were anchored to pylons, so the entire buoy apparatus rose and fell along a straight vertical line ensuring the buoys/lx sensors were not tilting with flow. In the UMR, there was not a suitable location to anchor along a vertical pylon. However, water level did not fluctuate over a wide range during the study period (Table 1) and field observations confirmed the buoys were not tilting except for a few days in the downstream location, which were removed from analysis. Data were recorded every 5 min and totaled 70 d and 63 d in the NR upstream and downstream reaches, respectively, and 20 d and 13 d in the UMR upstream and downstream reaches, respectively. Simultaneous light measurements from drifters and buoys were not available for all deployment dates due to equipment malfunctions and storms.

Additional light profiles were collected to show the relationship between PAR and lux (Supporting Information Fig. S1) and estimate reflection at the water surface. Conventional, manual light profiles from boats and docks under constant surface light were measured by lowering an upward facing PAR sensor (LICOR Quantum Sensor LI-190R, Nebraska, U.S.A.) and a lux sensor (HOBO) into the water to measure light at different depths. Reflection of lux at water surface was determined by measuring light just below and above the water surface and varied from 10% to 30% with a mean of 22% (n = 20). HOBO lux sensors were compared and showed a similar response to sunlight with paired sensors being within 0–12% error (Supporting Information Fig. S4), which was accounted for in uncertainty analysis of fixed-site light attenuation.

Fixed-site light attenuation

We also calculated light attenuation over time to test how well fixed-site measurements and optical theory predict light along flowpaths. Buoys measured light at two depths; therefore, we calculated fixed-site K_d by rearranging Eq. 1 to represent two spatially discrete depths (E_2 and E_1) in the water column rather than a profile (Davies-Colley and Nagels 2008);

$$K_d = \frac{\ln(E_2/E_1)}{\Delta z} \quad (5)$$

where E_2 is the light at the shallower depth (lux), E_1 is light at the deeper depth (lux), and Δz is the difference in the depth

between the two sensors. To minimize the effects of solar zenith angle, K_d was only calculated during mid-day time period, 10:30–16:30 h solar time (Miller and McPherson 1995; Zheng et al. 2002; Squires and Lesack 2003). Calculating K_d from light recorded at 5-min intervals was noisy due to naturally fluctuating underwater light conditions, anthropogenic disturbance, sensor error, and slight movements in sensor position. The resulting noise in K_d was smoothed with a moving average applied to each day of fixed-site K_d (Supporting Information Fig. S5). The uncertainty in fixed-site K_d was estimated using the propagation law of uncertainty ignoring the uncertainty in depth (Zheng et al. 2002);

$$u(K_d) = \sqrt{\left(\frac{1}{z_2 - z_1}\right)^2 \left(\frac{u_1}{E_d(z_1)}\right)^2 + \left(\frac{1}{z_2 - z_1}\right)^2 \left(\frac{u_2}{E_d(z_2)}\right)^2} \quad (6)$$

where u_1 is the uncertainty in light (E_d) measured at depth 1, or z_1, and u_2 is the uncertainty measured at depth 2, or z_2, and both u_1 and u_2 were assumed to be 12%. The estimated uncertainty differed depending on depth intervals over which K_d was measured at the different buoys, either 0.5, 0.75, or 1 m. The uncertainty in K_d for all measurements at the upstream NR buoy and downstream UMR buoy was $\pm$ 0.17 m^{-1}, $\pm$ 0.23 m^{-1} at the upstream UMR buoy, and $\pm$ 0.33 m^{-1} at the downstream NR buoy.

Analysis

Drifter behavior

We analyzed time series of drifter depths for characteristics of an autoregressive processes as indicators of random, turbulent fluctuations. If random, the autocorrelation function should show a strong correlation at a lag of one-time step with exponentially decreasing correlations with increasing lag. In addition, the differences between successive depths should be normally distributed (Rodean 1996; Faranda et al. 2014). During deployments with two drifters, the cross-correlation function was used to evaluate if the time series of drifter depths was constrained by spatial variability in channel depth. If two drifter depth time series showed strong correlations at lags equal to the difference between the release time of the two drifters, it was interpreted that the mean drifter flowpaths were mirroring changes in channel depth.

Light variability

We characterized the variability in light along flowpaths by calculating the frequency, duration, and interarrival time of "sunflecks" similar to how light variability has been characterized in the understory of forests (Chazdon and Pearcy 1991). Following the literature of forest ecology and plant physiology, a sunfleck was defined as continuous period of time above a light threshold important to photosynthesis. In the aquatic environment, an analogous threshold could be considered the compensation irradiance, typically a function of water depth, at which there is no net carbon gain because photosynthesis is equal to respiration (Wetzel 2001; Banse 2004). To explore how this sunfleck phenomenon could be applied to temporal variability in underwater light along flowpaths, we assumed a compensation irradiance of 500 lx (~ 10 μmol photon m^{-2} s^{-1} of PAR) based on previous lab and field experiments (Höglund and Landberg 1936; Pettersson 1938; Wetzel 2001; Banse 2004). Integrating the time series of light along flowpaths, we identified sunflecks and calculated their duration (min), interarrival time or periods of relative "darkness" (min), and the integrated or cumulative light for each event (lux). Like droughts or precipitation events (Chow and Kareliotis 1970), light exposure along flowpaths is a stochastic process where the duration and interarrival times of sunflecks can be described by an exponential distribution. Therefore, the mean sunfleck interarrival time and duration was estimated by fitting an exponential distribution, using the fitdistrplus R package (Delignette-Muller and Dutang 2015) and maximum likelihood method, and taking the inverse of the fitted shape parameter (λ).

To compare light variability between flowpaths and fixed-sites, we calculated summary statistics as well the cumulative light measured by drifters and buoys during each day. We focused on the variability in light using the coefficient of variation (CV) and the Richards-Baker (RB) flashiness index (Baker et al. 2004), metrics that are commonly used to quantify streamflow flashiness. Fixed-site summary statistics and cumulative light were calculated over the exact time period corresponding to the Lagrangian drifter deployment as well as over each daylight period. Daylight period is defined as the time period from morning to evening over which a fixed-site sensor at a given depth records nonzero light values. For some comparisons, like cumulative light, the same time period must be compared between flowpaths and fixed-sites. To compare light variability (i.e., CV and RB index), we compared the entire daylight period from a fixed-site (8–16 h) with the drifter deployments during daylight hours, which were generally shorter (3–8 h). Using the entire daylight period from fixed-sites increased the sample size of fixed-site days (i.e., data collected during nondeployment days) and captured the full diel variability in light at a fixed-site for a more robust comparison with drifter deployments.

We tested for differences in light variability between flowpaths and fixed-sites by grouping measurements of daily CV and the RB index by treatment, where treatments groups are drifters, buoys at 0 m, buoys at 0.5 m, buoys at 1 m, and buoys at 1.5 m depth. Statistical significance was tested first using ANOVA followed by post hoc pairwise comparisons between all treatment groups using Tukey's honest significant difference test.

Evaluating optical theory with Lagrangian measurements

We empirically assessed how well fixed-site measurements combined with optical theory (Eqs. 1, 2) model both the mean light exposure as well as the cumulative light exposure of

suspended particles. First, we modeled the mean light exposure using fixed-site measurements collected over the same time period as the corresponding drifter to which the mean light exposure was compared. We populated Eq. 2 with mean light at the water surface, $E_d(0)$, measured by fixed-site buoys corrected for surface reflection (assumed the mean reflection of 22%), mean K_d measured from fixed-site buoys and drifters, and the mean channel depth from manual measurements. We also applied this same model to cumulative light exposure, replacing the mean light at the water surface and mean light measured by drifters with the cumulative light. An uncertainty envelope was calculated assuming a 12% error in mean light at the water surface, a $\pm$ 0.23 m^{-1} uncertainty in K_d, and 15% error in mean channel depth.

Second, we tested if adding more temporal information, such as how light at the water surface, K_d, and depth of suspended particles changed over time, reduced the differences between modeled and measured cumulative light exposure compared to the previous modeling exercise. We compared the cumulative light measured during drifter deployments with three model scenarios. The first scenario assumed K_d was constant over space and time using the mean K_d measured by fixed-site buoys, the second also assumed a constant mean K_d but measured by drifters, and the third assumed a temporally variable K_d measured by fixed-site buoys. We then modeled cumulative light along flowpaths using Eq. 1 and temporal measurements of light at the water surface from fixed-site buoys, $E_d(0)$, corrected for surface reflection, K_d from fixed-site buoys or drifters, and depth over time measured by drifters (z). An uncertainty envelope was calculated assuming a 12% error in light measurements and a $\pm$ 0.23 m^{-1} uncertainty in K_d. We recognize we do not know the light at the water surface at every sampling time and location along drifter flowpaths; however, that is part of this exercise, to test if fixed-site measurements are representative of light along flowpaths. Additionally, in the UMR, riparian shading had little effect on light at the water surface along flowpaths since this site has few trees and is very open. The percent difference was calculated between measured and modeled scenarios for the deployments with the required data. Six deployments on the UMR met the data requirements: continuous, Lagrangian drifter data and continuous buoy data of both light at the surface and K_d. All analyses were performed in R statistical software (R 3.3.4).

Results

Drifter behavior

Drifters sampled a wide range of water depths and showed evidence of random, turbulent depth fluctuations. The depth time series had characteristics of an autoregressive process: a highly correlated time series at a lag of one-time step (autocorrelation function; ACF coefficients = 0.68–0.9), exponentially decreasing correlation coefficients with increasing time lag, and normally distributed differences between sequential depths along flowpaths (Supporting Information Figs. S6–S8). The depth distribution within a deployment was consistently log-normal across all deployments with modal depths between 1 and 2.9 m (approximately half of the mean channel depths of 2–6 m), indicating neutral buoyancy was maintained with infrequent depth excursions into deep pools up to 9.3 m (Fig. 3).

When multiple drifters were deployed in the UMR, they followed a similar path of depth within the water column vs. distance downstream for both simultaneously and staggered released deployments (Supporting Information Fig. S7). The cross-correlation function between the depth time series of two drifters deployed the same day had maximum correlations at lag times approximately equal to the release time offset (Supporting Information Table S1), suggesting the drifters responded similarly to large scale turbulent fluctuations likely dictated by spatial patterns in channel depth, planform morphology, and potentially secondary currents (Rutherford 1994).

Light variability

Light along flowpaths was highly variable (Fig. 4, Supporting Information Fig. S9). Sunflecks, or continuous periods where light was > 500 lx, accounted for 62–99% of the cumulative light during drifter deployments measuring between 3 and 90 sunflecks per deployment. Combining all the sunflecks from all deployments, most individual sunflecks (70%) were above

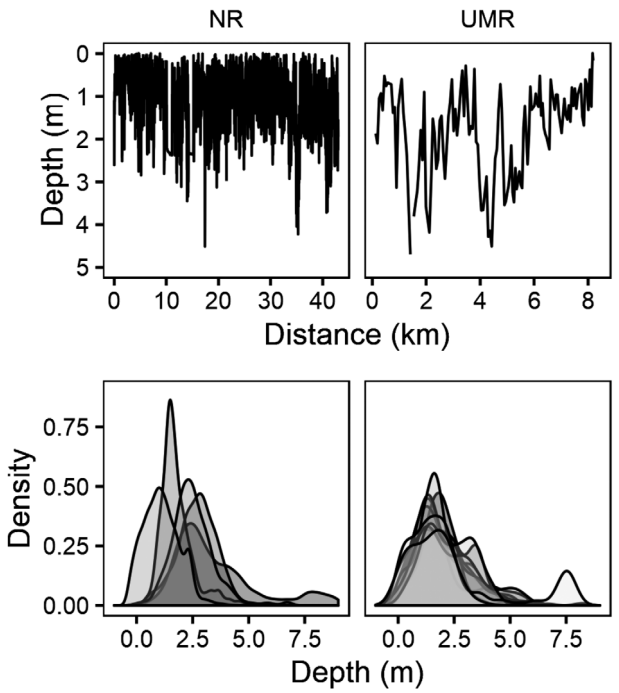

Fig. 3. (Top) The drifter depth vs. distance downstream from one example flowpath along each river (UMR and NR), (Bottom) the log-normal frequency distribution of depths along flowpaths for each drifter deployment in the UMR and NR. See Supporting Information for more time series of drifter depths.

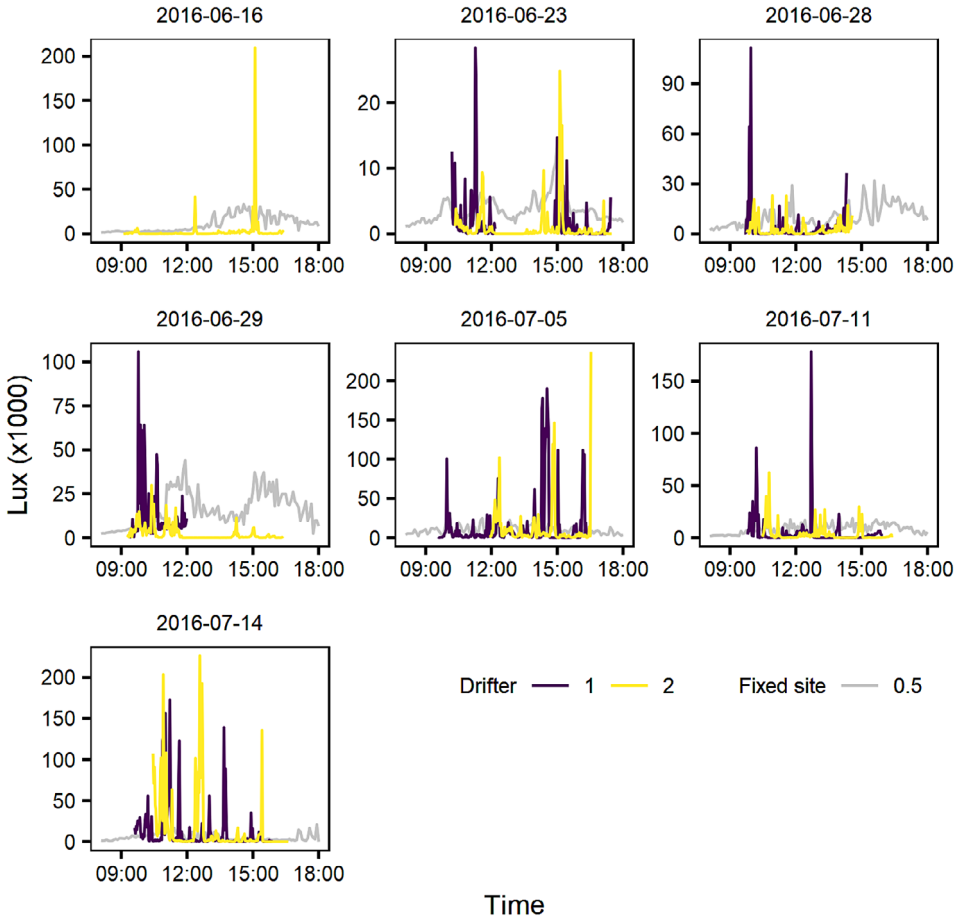

Fig. 4. The stochastic nature of light exposure along flowpaths. Example of light (lux) measured by neutrally buoyant drifters over time during deployments in the UMR. Multiple lines (colors) indicate multiple drifters on the same day. The gray line shows light at a fixed-site buoy at 0.5 m depth for reference. Note the axes have different ranges for each plot. See Supporting Information for time series on the NR. [Color figure can be viewed at wileyonlinelibrary.com]

the 1:1 line when plotting the proportion of cumulative light vs. proportion of cumulative deployment time, showing the importance of individual sunflecks on cumulative light exposure (Fig. 5). For example, in the most extreme case, a 1-min sunfleck accounted for 17% of the cumulative light in just 0.2% of the deployment time for one drifter deployment on the NR. Combining sunflecks across deployments within each river, the mean sunfleck interarrival time, estimated by fitting exponential distributions, was 12 min and 6.8 min in the UMR and NR, respectively, and the mean sunfleck duration was 14 min and 1.6 min in the UMR and NR, respectively (Fig. 6). Note that measuring sunflecks may be sensitive to the sensor measurement frequency, which was 0.5 min in the NR and 2 min in the UMR, likely contributing the shorter duration and interarrival time on the NR in addition to the generally deeper channels and darker waters in the NR.

Light was more variable along flowpaths than over time at fixed-sites. ANOVA followed by a post hoc pairwise comparisons using Tukey's honest significant difference test showed that the CV and RB flashiness index were both significantly higher ($p \leq 1 \times 10^{-14}$) during drifter deployments compared to fixed-site buoys at any depth for both rivers (Fig. 7, Supporting Information Fig. S10, Tables S2, S3). During the daylight period at a fixed-site, light typically had a CV of 1 across rivers, buoys, and depths while the CV of light measured by drifters was typically three times higher (Fig. 7).

Spatial variability in light attenuation

Drifters detected longitudinal variability in K_d at the kilometer scale. Despite the error in drifter K_d measurements, ranging from $\pm$ 0.04 to 0.57 m^{-1} in the NR and $\pm$ 0.05 to 0.94 m^{-1} in the UMR, there were detectable differences in K_d every 1–2 km along the UMR and NR (Fig. 8, Supporting Information Fig. S11). Drifters in the UMR, whether they were released simultaneously or staggered (on 7/11 and 7/14), showed similar spatial patterns in K_d, suggesting K_d was affected by consistent spatial variability in optical water quality (CDOM, suspended sediment, phytoplankton) and/or the depths over which drifters measured K_d (Fig. 8).

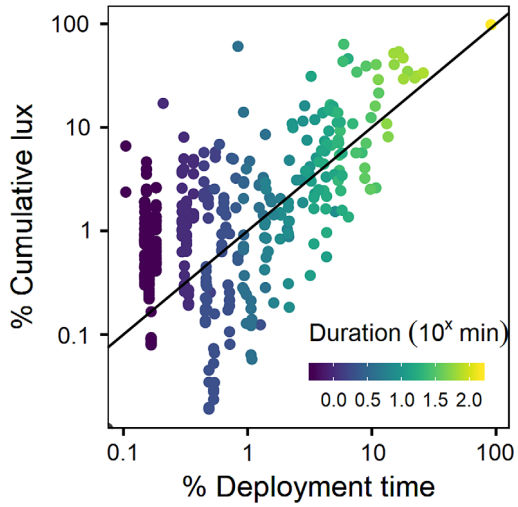

Fig. 5. Sunflecks (i.e., exceeding 500 lx) accounted for a disproportionate amount of the cumulative light exposure during drifter deployments, with 70% of sunflecks lying above the 1:1 line of percentage of cumulative lux vs. percentage of total deployment time accounted for by each sunfleck. Each point is an individual sunfleck, and this plot shows all sunflecks from the all drifter deployments across both rivers. [Color figure can be viewed at wileyonlinelibrary.com]

We tested if changes in K_d along a river could be explained by the depth of drifter measurements, in other words, vertical variability in K_d in the water column. Theoretically, there should be a small, typically negligible, decrease in K_d with depth from the water surface (Kirk 1994). Linear regressions of

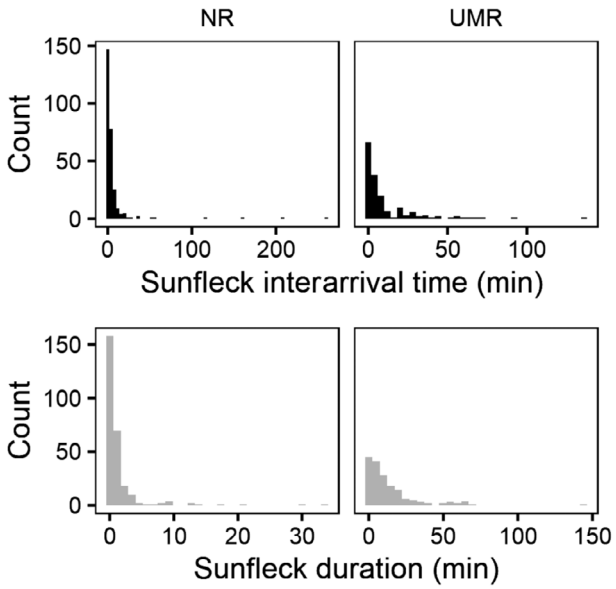

Fig. 6. Interarrival time (top) and duration (bottom) of sunflecks (i.e., exceeding 500 lx) for all sunflecks from all drifter deployments within each river, the UMR and NR. Fitting exponential distributions shows that the mean interarrival time was 12 min in UMR and 6.8 min in NR, and the mean duration was 14 min in the UMR and 1.6 min in the NR.

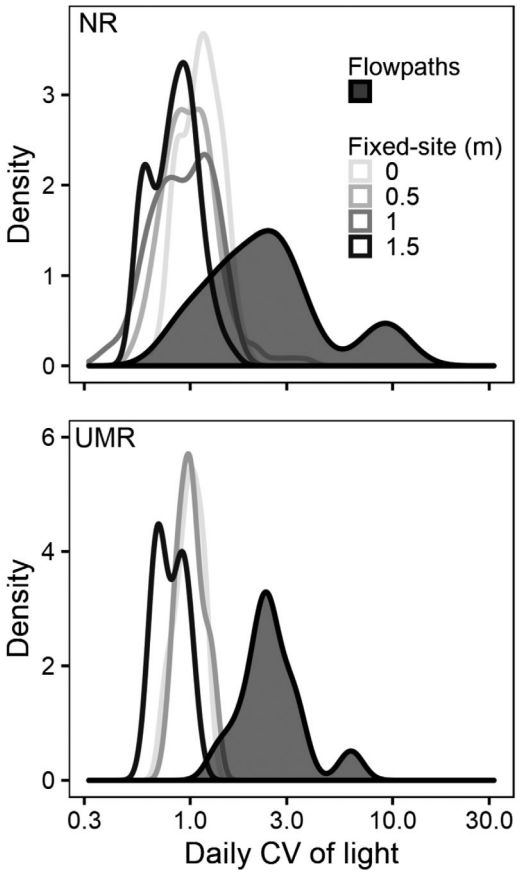

Fig. 7. The coefficient of variation of light (lux) along flowpaths was always higher than the CV of light at a fixed-site buoy at any depth during daylight hours. Shown here is the distribution of CVs during all flowpath deployments compared to the daily CV from fixed-sites grouped by depth below the water surface in both the NR and UMR.

K_d vs. depth showed 35% (6 of 17, combining the UMR and NR) of deployments with the required data had a significant decrease ($p = 0.02\times 10^{-12}$ to 0.6×10^{-12}) in K_d with increasing water depth. Of the deployments with significant K_d-depth correlations, between 1% and 47% of the variance in K_d (R^2 ranging from 0.01 to 0.47) was explained by depth (Supporting Information Figs. S13, S14). The lack of strong correlations between K_d and depth during most deployments was further evidence that there were longitudinal changes in K_d, that may have affected the variability in light exposure along flowpaths.

Evaluating optical theory with Lagrangian measurements

Fixed-site measurements combined with optical theory predicted a consistently higher light exposure compared to drifter measurements, suggesting suspended particles in our study reaches experienced darker conditions than optical theory would predict. The modeled mean light exposure was between 61% and 1700% higher than the measured mean light exposure using mean conditions (although with high uncertainty in modeled mean light, Supporting Information Table S4).

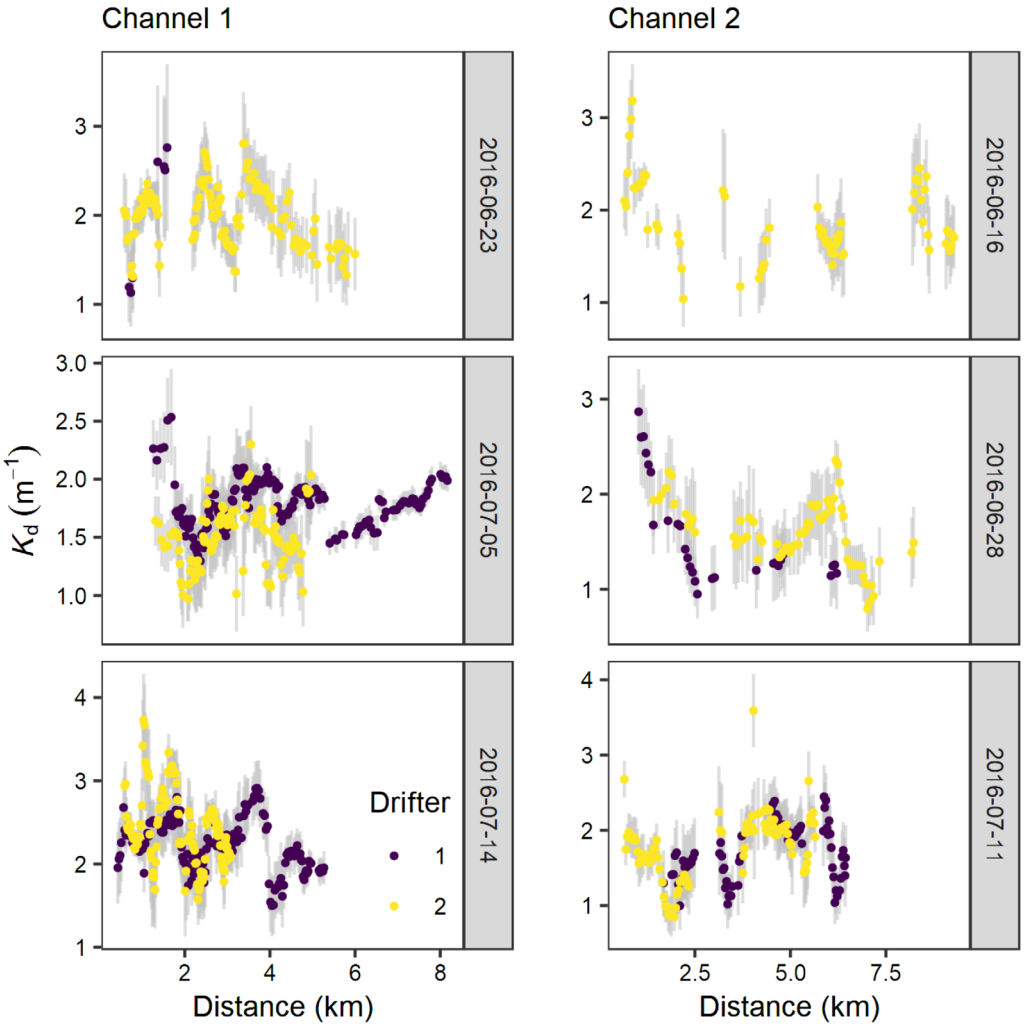

Fig. 8. Similar spatial patterns in light attenuation (K_d) vs. distance downstream measured along the UMR channels 1 and 2 by drifters. Different colors show multiple drifters. Each point is the K_d measured over a 30-min window and the bars show the error for each measurement. Note the similar spatial patterns for multiple drifters and even during different dates in channel 2. See Supporting Information for data from the NR. [Color figure can be viewed at wileyonlinelibrary.com]

Similarly, the modeled cumulative light exposure was between 56% and 1686% higher than the measured cumulative light exposure using mean conditions (also note the high uncertainty in the modeled cumulative light, Table 2).

Modeling the cumulative light exposure with temporally variable conditions in light at the water surface and depth along a flowpath reduced the bias between modeled and measured values; however, modeled cumulative light exposure remained between 90% and 290% higher than measured (Table 3; Fig. 9). There was no difference in cumulative light exposure when assuming a constant K_d (measured by buoys or drifters) vs. a temporally variable K_d, at least during the six experiments in the UMR with the required data. While there was considerable uncertainty in the modeled and measured cumulative light, the uncertainty bounds did not overlap (Fig. 9), and it is the consistent direction of the bias rather than the magnitude of the bias that has important implications for how to quantify underwater light in rivers.

Discussion

In our study sites, light varied more along flowpaths than over time at fixed-sites (Fig. 7), cumulative light exposure along flowpaths was dominated by sunflecks (Fig. 5), and fixed-site measurements combined with optical theory consistently overestimated the light exposure of suspended particles during downstream transport (Fig. 9). It was no surprise that vertical mixing in a river caused suspended particles to experience rapid shifts in light; however, our results have important implications for how to quantify underwater light and its effects on photo-reactive processes in rivers. First, our results showed that suspended organisms experience different and

Table 2. Comparing the measured cumulative light exposure (lux) by drifters with the modeled cumulative light exposure using fixed-site measurements and optical theory assuming mean conditions according to Eq. 2. *U* is the +/− uncertainty in each of the measured and modeled values, and the percent difference between modeled and measured on the right showed modeled light exposure was consistently higher than measured.

	Measured and modeled cumulative flowpath lux (using mean conditions for modeling)						Percent difference between modeled and measured	
Deployment date	Measured	*U*	Modeled (buoy K_d)	*U*	Modeled (drifter K_d)	*U*	Modeled (buoy K_d)	Modeled (drifter K_d)
16 Jun 2016	1.0×10^6	12%	5.6×10^6	47%	5.7×10^6	47%	440	443
23 Jun 2016	4.4×10^5	12%	2.3×10^6	47%	2.0×10^6	46%	428	344
28 Jun 2016	1.0×10^6	12%	3.5×10^6	48%	3.9×10^6	49%	246	285
28 Jun 2016	7.3×10^5	12%	3.7×10^6	48%	4.0×10^6	49%	406	445
29 Jun 2016	2.0×10^6	12%	3.1×10^6	43%	4.3×10^6	45%	56	114
29 Jun 2016	8.7×10^5	12%	1.4×10^7	46%	1.6×10^7	47%	1544	1686

more variable light regimes than organisms on, or rooted to, the riverbed. Second, our flowpath measurements could help parameterize the variability in light exposure of suspended particles in future laboratory and modeling studies. Third, quantifying light exposure of suspended particles during downstream transport may require more spatially explicit, and/or flowpath-based approaches considering the bias between modeled and measured light exposure.

While there are a variety of approaches that simulate light exposure of suspended particles due to turbulent mixing, our flowpath measurements can inform more realistic experimental and modeling approaches for variable light and how it effects photo-reactive processes. Experimental approaches often use periodic oscillations in light (Mallin and Paerl 1992) and modeling approaches often assume instantaneous mixing of a population of suspended particles exposed to depth-averaged light (Sellers and Bukaveckas 2003; Ross and Sharples 2004). These approaches are useful for understanding the aggregate response of a population to mean conditions, but our results indicate that individual organisms experience highly variable conditions that are much different from the mean. Our data suggest that experiments can randomly oscillate light between limiting and nonlimiting conditions for photosynthesis on the timescale of minutes according to exponential distributions with a mean duration of nonlimiting conditions (e.g., sunflecks) of 1.6–14 min and a mean duration of limiting conditions of 6.8–12 min. The duration and interarrival time of sunflecks implied phytoplankton in the river reaches we studied must ramp-up photosynthesis for 1.6–14 min, on average, following a period of low light lasting 6.8–12 min, on average. Given that sunflecks account for a disproportionate amount of the cumulative light exposure along flowpaths, quantifying how sunfleck frequency, magnitude, and duration affects photosynthetic processes may provide a more robust understanding of primary production in rivers at the temporal scales relevant to physiological response (Chazdon and Pearcy 1991).

While we predicted that modeled light exposure, using fixed-site measurements combined with optical theory, would be different than the light exposure measured along flowpaths, it was

Table 3. Comparing the measured cumulative light exposure (lux) by drifters with the modeled cumulative light exposure using fixed-site measurements and optical theory assuming temporally variable depth, light at the surface, and K_d. The three scenarios: Constant K_d (mean K_d measured by a buoy), constant K_d (mean K_d measured by the drifter), and temporally variable K_d (measured by a buoy). *U* +/− is the uncertainty in each of the measured and modeled values, and the percent difference between modeled and measured on the right showed modeled light exposure was consistently higher than measured.

	Measured and modeled cumulative flowpath lux (using temporally variable data for modeling)								Percent difference between modeled and measured		
Deployment date	Measured	*U*	Modeled constant *K*d (buoy)	*U*	Modeled constant *K*d (drifter)	*U*	Modeled variable K_d	*U*	Modeled constant K_d (buoy)	Modeled constant K_d (drifter)	Modeled variable K_d
16 Jun 2016	1.0×10^6	12%	2.1×10^6	39%	2.4×10^6	90%	2.1×10^6	39%	102	136	101
23 Jun 2016	4.4×10^5	12%	1.1×10^6	34%	8.4×10^5	42%	1.1×10^6	35%	150	90	157
28 Jun 2016	1.0×10^6	12%	2.3×10^6	32%	3.3×10^6	69%	2.4×10^6	32%	126	227	131
28 Jun 2016	7.3×10^5	12%	2.2×10^6	36%	2.7×10^6	70%	2.2×10^6	36%	199	268	206
29 Jun 2016	1.9×10^6	12%	7.0×10^6	18%	7.7×10^6	47%	6.9×10^6	18%	259	295	257
29 Jun 2016	8.1×10^5	12%	2.2×10^6	39%	2.6×10^6	50%	3.2×10^6	73%	175	219	290

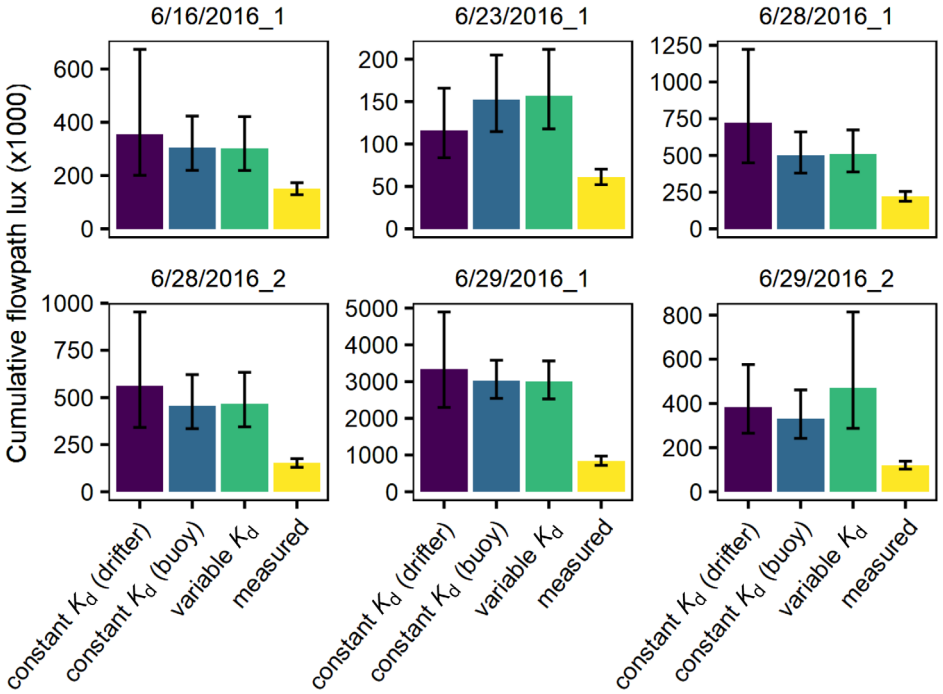

Fig. 9. The measured cumulative light (lux) along flowpaths was consistently lower than the modeled cumulative light across all six deployments with sufficient data. Each plot shows an individual drifter deployment, some from the same date which means there were two drifters. Cumulative light was modeled using measured drifter depths, fixed-site measurements of light at the water surface, and K_d measured from buoys and drifters under the assumptions of a constant K_d over time and variable K_d over time. [Color figure can be viewed at wileyonlinelibrary.com]

surprising that both the measured mean and cumulative light exposure were consistently lower than modeled. If the measured light exposure was higher than modeled light exposure in this study, it would have supported prior hypotheses for why phytoplankton persist in large, optically deep rivers. These hypotheses include the added retention time in slow-flowing channel margins and backwater habitats (Walks 2007; Ochs et al. 2013) and diffusive dispersal (Speirs and Gurney 2001). While our findings do not help resolve this paradox, they do point to the importance of sunflecks and vertical mixing as critical sources of light for photo-reactive processes in large rivers.

One explanation for the bias between modeled and measured light exposure along flowpaths is the "fallacy of the average," or Jensen's inequality, which mathematically shows that averaging over a nonlinear function will introduce bias (Ruel and Ayres 1999; Denny 2017). While Jensen's inequality is typically invoked in the nonlinear response of biological phenomenon to physical drivers, such as photosynthesis as a nonlinear, saturating function of light, light is also a nonlinear function of depth. Therefore, simple mathematics confirms that the depth-averaged light exposure should overestimate the actual light exposure of a suspended particle.

Taking our results together, spatial changes along flowpaths were critical to light exposure of suspended particles in our study reaches, further explaining the bias between measured and modeled light exposure. Spatial changes include the distribution of depths experienced by a suspended particle during downstream transport and the spatial–temporal changes in light attenuation and/or light at the water surface along a flowpath.

Spatial variability in water depth (i.e., channel morphology) is a dominant control of light exposure for suspended particles (Sellers and Bukaveckas 2003), and multiple results further supported this conclusion. The bias between measured and modeled cumulative light was reduced by half or more in all but one case, when the exact sequence of water depths was used rather than the mean mixing depth to model light exposure (Tables 2–3). The log-normal distribution of drifter depths suggested that the river reaches had deep and shallow sections as the drifters were occasionally mixed into deep pools with low light conditions (Figs. 3–4). In deeper reaches, suspended particles can mix to greater depths where the velocity is lower thus increasing the time spent under low light conditions. The variability in water depth, and corresponding time spent at different water depths, should be accounted for in light exposure of suspended particles.

In addition, the convolution of external light filters (e.g., channel orientation, clouds, riparian shading, topography), internal light filters (e.g., suspended sediment, phytoplankton, CDOM), and how they overlap with the timing, longitudinal, and vertical position of a suspended particle during downstream transport may also be important to light exposure. Our

results suggested that fixed-site measurements, regardless of assumptions of constant or temporally variable conditions, were not representative of spatial changes in K_d and light at the water surface in our study reaches. Modeled cumulative light exposure was still greater than measured after accounting for the distribution of depths experienced by a suspended particle using both a mean K_d and a temporally variable K_d. The drifters indeed measured spatial variability in K_d along the reaches that was not captured by fixed-site measurements. These results highlighted that matching measurement approach with how the object of study experiences its environment (e.g., is it advected downstream or mostly stationary) should be considered when quantifying light exposure.

To represent the variability in light and the cumulative light exposure of suspended particles during downstream transport, it is important to consider temporal and spatial effects on underwater light along a river. Spatially explicit and/or flowpath approaches are needed for measuring and modeling light exposure and photo-reactive processes in rivers (Minor et al. 2013), which can provide new insights into how organisms and ecosystems respond to variability in environmental conditions (Doyle and Ensign 2009; Hellweger et al. 2014; Doblin and Van Sebille 2016; Ensign et al. 2017). Future work on the effect of light on the quantity and composition of phytoplankton, nutrients, dissolved organic matter, and contaminants in rivers, all of which can behave as suspended particles, should consider light variability on time scales of minutes and account for the potential bias in light exposure estimated by fixed-site measurements and optical theory.

References

Baker, D. B., R. P. Richards, T. T. Loftus, and J. W. Kramer. 2004. A new flashiness index: Characteristics and applications to Midwestern rivers and streams. J. Am. Water Resour. Assoc. **40**: 503–522. doi:10.1111/j.1752-1688.2004.tb01046.x

Banse, K. 2004. Should we continue to use the 1% light depth convention for estimating the compensation depth of phytoplankton for another 70 years? Limnol. Oceanogr.: Bull. **13**: 49–52. doi:10.1002/lob.200413349

Chazdon, R. L. 1988. Sunflecks and their importance to forest understorey plants, Vol. 18 p. 1–63. *In* David A. Bohan and Alex J. Dumbrell [eds.], Advances in ecological research. Elsevier.

Chazdon, R. L., and N. Fetcher. 1984. Photosynthetic light environments in a lowland tropical rain forest in Costa Rica. J. Ecol. **72**: 553–564. doi:10.2307/2260066

Chazdon, R. L., and R. W. Pearcy. 1991. The importance of sunflecks for forest understory plants. Bioscience **41**: 760–766. doi:10.2307/1311725

Chow, V. T., and S. Kareliotis. 1970. Analysis of stochastic hydrologic systems. Water Resour. Res. **6**: 1569–1582. doi:10.1029/WR006i006p01569

Cory, R. M., C. P. Ward, B. C. Crump, and G. W. Kling. 2014. Sunlight controls water column processing of carbon in arctic fresh waters. Science **345**: 925–928. doi:10.1126/science.1253119

D'Asaro, E. A. 2003. Performance of autonomous Lagrangian floats. J. Atmos. Ocean. Technol. **20**: 896–911. doi:10.1175/1520-0426(2003)020<0896:POALF>2.0.CO;2

D'Asaro, E. A., D. M. Farmer, J. T. Osse, and G. T. Dairiki. 1996. A Lagrangian float. J. Atmos. Ocean. Technol. **13**: 1230–1246. doi:10.1175/1520-0426(1996)013<1230:ALF>2.0.CO;2

Davies-Colley, R., W. Vant, and G. Latimer. 1984. Optical characterisation of natural waters by PAR measurement under changeable light conditions. N. Z. J. Mar. Freshw. Res. **18**: 455–460. doi:10.1080/00288330.1984.9516067

Davies-Colley, R. J. 1990. Frequency distributions of visual water clarity in 12 New Zealand rivers. N. Z. J. Mar. Freshw. Res. **24**: 453–460. doi:10.1080/00288330.1990.9516436

Davies-Colley, R. J., and J. M. Quinn. 1998. Stream lighting in five regions of North Island, New Zealand: Control by channel size and riparian vegetation. N. Z. J. Mar. Freshw. Res. **32**: 591–605. doi:10.1080/00288330.1998.9516847

Davies-Colley, R. J., and J. W. Nagels. 2008. Predicting light penetration into river waters. J. Geophys. Res. **113**: 1–9. doi:10.1029/2008JG000722

Delignette-Muller, M. L., and C. Dutang. 2015. fitdistrplus: An R Package for fitting distributions. J. Stat. Softw. **64**: 34.

DeNicola, M., K. D. Hoagland, and S. C. Roemer. 1992. Influences of canopy cover on spectral irradiance and periphyton assemblages in a prairie stream. J. North Am. Benthol. Soc. **11**: 391–404. doi:10.2307/1467560

Denny, M. 2017. The fallacy of the average: On the ubiquity, utility and continuing novelty of Jensen's inequality. J. Exp. Biol. **220**: 139–146. doi:10.1242/jeb.140368

Descy, J.-P., and V. Gosselain. 1994. Development and ecological importance of phytoplankton in a large lowland river (River Meuse, Belgium), p. 139–155. *In* J.-P. Descy, C. S. Reynolds and J. Padisdk [eds.], Phytoplankton in turbid environments: Rivers and shallow lakes. Belgium: Kluwer Academic Publishers, Springer.

Doblin, M. A., and E. Van Sebille. 2016. Drift in ocean currents impacts intergenerational microbial exposure to temperature. Proc. Natl. Acad. Sci. USA **113**: 5700–5705. doi:10.1073/pnas.1521093113

Doi, H. 2009. Spatial patterns of autochthonous and allochthonous resources in aquatic food webs. Popul. Ecol. **51**: 57–64. doi:10.1007/s10144-008-0127-z

Doyle, M. W., and S. H. Ensign. 2009. Alternative reference frames in river system science. Bioscience **59**: 499–510. doi:10.1525/bio.2009.59.6.8

Ensign, S. H., M. W. Doyle, and J. R. Gardner. 2017. New strategies for measuring rates of environmental processes in rivers, lakes, and estuaries. Freshw. Sci. **36**: 453–465. doi:10.1086/692998

Falkowski, P. G. 1984. Physiological responses of phytoplankton to natural light regimes. J. Plankton Res. **6**: 295–307. doi:10.1093/plankt/6.2.295

Faranda, D., and others. 2014. Modelling and analysis of turbulent datasets using Auto Regressive Moving Average processes. Phys. Fluids **26**: 105101. doi:10.1063/1.4896637

Gordon, H. R. 1989. Can the Lambert-Beer law be applied to the diffuse attenuation coefficient of ocean water? Limnol. Oceanogr. **34**: 1389–1409. doi:10.4319/lo.1989.34.8.1389

Hall, R. O., and others. 2015. Turbidity, light, temperature, and hydropeaking control primary productivity in the Colorado River, Grand Canyon. Limnol. Oceanogr. **60**: 512–526. doi:10.1002/lno.10031

Heaston, E. D., M. J. Kaylor, and D. R. Warren. 2017. Characterizing short-term light dynamics in forested headwater streams. Freshw. Sci. **36**: 259–271. doi:10.1086/691540

Hellweger, F. L., E. van Sebille, and N. D. Fredrick. 2014. Biogeographic patterns in ocean microbes emerge in a neutral agent-based model. Science **345**: 1346–1349. doi:10.1126/science.1254421

Hillebrand, H. 2005. Light regime and consumer control of autotrophic biomass. J. Ecol. **93**: 758–769. doi:10.1111/j.1365-2745.2005.00978.x

Höglund, H., and S. Landberg. 1936. Further investigations upon the photosynthesis of phyto-plankton by constant illumination. Rapp. Proc. Verb. Cons. Int. Explor. Mer. **95**: 32–33.

Jirka, G. H. 2001. Large scale flow structures and mixing processes in shallow flows. J. Hydraul. Res. **39**: 567–573. doi:10.1080/00221686.2001.9628285

Julian, J. P., M. W. Doyle, S. M. Powers, E. H. Stanley, and J. A. Riggsbee. 2008*a*. Optical water quality in rivers. Water Resour. Res. **44**: 1–19. doi:10.1029/2007WR006457

Julian, J. P., M. W. Doyle, and E. H. Stanley. 2008*b*. Empirical modeling of light availability in rivers. J. Geophys. Res. Biogeosci. **113**: 1–16. doi:10.1029/2007JG000601

Kirk, J. T. 1994. Light and photosynthesis in aquatic ecosystems. Cambridge Univ. Press.

Koch, R. W., D. L. Guelda, and P. A. Bukaveckas. 2004. Phytoplankton growth in the Ohio, Cumberland and Tennessee Rivers, USA: Inter-site differences in light and nutrient limitation. Aquat. Ecol. **38**: 17–26. doi:10.1023/B:AECO.0000021082.42784.03

Köhler, J., L. Wang, A. Guislain, and T. Shatwell. 2018. Influence of vertical mixing on light-dependency of phytoplankton growth. Limnol. Oceanogr. **63**: 1156–1167. doi:10.1002/lno.10761

Leakey, A., J. Scholes, and M. Press. 2004. Physiological and ecological significance of sunflecks for dipterocarp seedlings. J. Exp. Bot. **56**: 469–482. doi:10.1093/jxb/eri055

Leech, D., and S. Johnsen. 2009. Light, biological receptors, p. 671–681. *In* Gene E. Likens [ed.], Encyclopedia of inland waters, v. **2**. Amsterdam: Elsevier.

Leopold, L. B., and T. Maddock. 1953. The hydraulic geometry of stream channels and some phyriographic implications: Quantitative measurement of some of the hydraulic factors that help to determine the shape of natural stream channels: Depth, width, velocity, and suspended load, and how they vary with discharge as simple power functions; Teir Interrelations are Described by the Term "hydraulic Geometry". U.S. Government Printing Office.

Lien, R. C., and E. A. D'Asaro. 2006. Measurement of turbulent kinetic energy dissipation rate with a Lagrangian float. J. Atmos. Ocean. Technol. **23**: 964–976. doi:10.1175/JTECH1890.1

Litchman, E. 1998. Population and community responses of phytoplankton to fluctuating light. Oecologia **117**: 247–257. doi:10.1007/s004420050655

Litchman, E. 2000. Growth rates of phytoplankton under fluctuating light. Freshw. Biol. **44**: 223–235. doi:10.1046/j.1365-2427.2000.00559.x

Long, M. H., J. E. Rheuban, P. Berg, and J. C. Zieman. 2012. A comparison and correction of light intensity loggers to photosynthetically active radiation sensors. Limnol. Oceanogr.: Methods **10**: 416–424. doi:10.4319/lom.2012.10.416

Mallin, M. A., and H. W. Paerl. 1992. Effects of variable irradiance on phytoplankton productivity in shallow estuaries. Limnol. Oceanogr. **37**: 54–62. doi:10.4319/lo.1992.37.1.0054

Miller, R. L., and B. F. McPherson. 1995. Modeling photosynthetically active radiation in water of Tampa Bay, Florida, with emphasis on the geometry of incident irradiance. Estuar. Coast. Shelf Sci. **40**: 359–377. doi:10.1006/ecss.1995.0025

Minor, E. C., E. James, J. A. Austin, V. Nelson, R. Lusk, and K. Mopper. 2013. A preliminary examination of an in situ dual dye approach to measuring light fluxes in lotic systems. Limnol. Oceanogr.: Methods **11**: 631–642. doi:10.4319/lom.2013.11.631

Nadaoka, K., and H. Yagi. 1998. Shallow-water turbulence modeling and horizontal large-eddy computation of river flow. J. Hydraul. Eng. **124**: 493–500. doi:10.1061/(ASCE)0733-9429(1998)124:5(493)

Nelson, K. L., and others. 2018. Sunlight-mediated inactivation of health-relevant microorganisms in water: A review of mechanisms and modeling approaches. Environ. Sci. Process. Impacts **20**: 1089–1122. doi:10.1039/C8EM00047F

Ochs, C. A., O. Pongruktham, and P. V. Zimba. 2013. Darkness at the break of noon: Phytoplankton production in the Lower Mississippi River. Limnol. Oceanogr. **58**: 555–568. doi:10.4319/lo.2013.58.2.0555

Pearcy, R. W., and D. A. Way. 2012. Two decades of sunfleck research: Looking back to move forward. Oxford Univ. Press.

Pettersson, H. 1938. Measurements of the angular distribution of submarine light. Rapp. Cons. Explor. Mer. **108**: 9.

Phlips, E., M. Cichra, F. Aldridge, J. Jembeck, J. Hendrickson, and R. Brody. 2000. Light availability and variations in phytoplankton standing crops in a nutrient-rich blackwater river. Limnol. Oceanogr. **45**: 916–929. doi:10.4319/lo.2000.45.4.0916

Reynolds, C. 1990. Temporal scales of variability in pelagic environments and the response of phytoplankton. Freshw. Biol. **23**: 25–53. doi:10.1111/j.1365-2427.1990.tb00252.x

Reynolds, C. S. 2006. The ecology of phytoplankton. Cambridge Univ. Press.

Reynolds, C. S., P. A. Carling, and K. J. Beven. 1991. Flow in river channels: New insights into hydraulic retention. *Archiv fur Hydrobiologie*. **121**:171–179. doi:10.1111/j.1749-6632.1991.tb24390.x.

Rodean, H. C. 1996. Stochastic Lagrangian models of turbulent diffusion. Springer.

Ross, O. N., and J. Sharples. 2004. Recipe for 1-D Lagrangian particle tracking models in space-varying diffusivity. Limnol. Oceanogr.: Methods **2**: 289–302. doi:10.4319/lom.2004.2.289

Ruel, J. J., and M. P. Ayres. 1999. Jensen's inequality predicts effects of environmental variation. Trends Ecol. Evol. **14**: 361–366. doi:10.1016/S0169-5347(99)01664-X

Rutherford, J. C. 1994. River mixing. Wiley.

Sellers, T., and P. A. Bukaveckas. 2003. Phytoplankton production in a large, regulated river: A modeling and mass balance assessment. Limnol. Oceanogr. **48**: 1476–1487. doi:10.4319/lo.2003.48.4.1476

Smith, D. G., R. J. Davies-Colley, J. Knoef, and G. W. Slot. 1997. Optical characteristics of New Zealand rivers in relation to flow. J. Am. Water Resour. Assoc. **33**: 301–312. doi:10.1111/j.1752-1688.1997.tb03511.x

Speirs, D. C., and W. S. Gurney. 2001. Population persistence in rivers and estuaries. Ecology **82**: 1219–1237. doi:10.1890/0012-9658(2001)082[1219:PPIRAE]2.0.CO;2

Squires, M. M., and L. F. Lesack. 2003. Spatial and temporal patterns of light attenuation among lakes of the Mackenzie Delta. Freshw. Biol. **48**: 1–20. doi:10.1046/j.1365-2427.2003.00960.x

Sverdrup, H. 1953. On conditions for the vernal blooming of phytoplankton. J. Cons. Int. Explor. Mer. **18**: 287–295.

Thorp, J. H., and M. D. Delong. 1994. The riverine productivity model: An heuristic view of carbon sources and organic processing in large river ecosystems. Oikos **70**: 305–308. doi:10.2307/3545642

Thorp, J. H., M. D. Delong, K. S. Greenwood, and A. F. Casper. 1998. Isotopic analysis of three food web theories in constricted and floodplain regions of a large river. Oecologia **117**: 551–563. doi:10.1007/s004420050692

Thorp, J. H., and M. D. Delong. 2002. Dominance of autochthonous autotrophic carbon in food webs of heterotrophic rivers. Oikos **96**: 543–550. doi:10.1034/j.1600-0706.2002.960315.x

Vähätalo, A. 2010. Light, photolytic reactivity and chemical products, p. 37–49. *In* G. E. Likens [ed.], Biogeochemistry of inland waters. Elsevier.

Walks, D. 2007. Persistence of plankton in flowing water. Can. J. Fish. Aquat. Sci. **64**: 1693–1702. doi:10.1139/f07-131

Way, D. A., and R. W. Pearcy. 2012. Sunflecks in trees and forests: From photosynthetic physiology to global change biology. Tree Physiol. **32**: 1066–1081. doi:10.1093/treephys/tps064

Wellnitz, T., and B. Rinne. 1999. Photosynthetic response of stream periphyton to fluctuating light regimes. J. Phycol. **35**: 667–672. doi:10.1046/j.1529-8817.1999.3540667.x

Wetzel, R. G. 2001. Limnology: Lake and river ecosystems. Gulf Professional Publishing.

Wilcox, D., U. Fish, and W. Service. 1993. An aquatic habitat classification system for the Upper Mississippi River System. Onalaska, Wisconsin: U.S. Fish and Wildlife Service, Environmental Management Technical Center.

Zheng, X., T. Dickey, and G. Chang. 2002. Variability of the downwelling diffuse attenuation coefficient with consideration of inelastic scattering. Appl. Opt. **41**: 6477–6488. doi:10.1364/AO.41.006477

Acknowledgments

We thank funding sources: NSF-IGERT(DGE-1068871), North Carolina SeaGrant minigrant, and the Nicholas School of the Environment; field support from the USGS-Upper Midwest Environmental Sciences Center, James Larson, Virginia Young, Chelsea Clifford, Matt Fuller; landowners along the Neuse River; comments on earlier drafts from Emily Bernhardt and Jim Heffernan; and for helpful reviews from Robert Hall, Christopher Rutherford, Robert Davies-Colley, Anssi Vahatalo, Kathi Jo Jankowski, and several other anonymous reviewers. Drifter data are available at https://github.com/johngardner87/FlowpathLight.

Conflict of Interest

None declared.

Submitted 31 October 2018
Revised 09 May 2019 and 18 June 2019
Accepted 27 June 2019

Associate editor: Bob Hall